Available online at www.sciencedirect.com
ScienceDirect
Microelectronic Engineering xxx (2006) xxx–xxx
MICROELECTRONIC ENGINEERING
www.elsevier.com/locate/mee

Local indentation modulus characterization via two contact resonance frequencies atomic force acoustic microscopy

D. Passeri [a,*], A. Bettucci [a], M. Germano [a], M. Rossi [a], A. Alippi [a], A. Fiori [b], E. Tamburri [b], S. Orlanducci [b], M.L. Terranova [b], J.J. Vlassak [c]

[a] *Dipartimento di Energetica, Università di Roma "La Sapienza", Via A. Scarpa 16, 00161 Roma, Italy*
[b] *Dipartimento di Scienze e Tecnologie Chimiche, Università di Roma "Tor Vergata" and Micro and Nano-structured Systems Laboratory (MINASlab), Via della Ricerca Scientifica, 00133 Roma, Italy*
[c] *Division of Engineering and Applied Sciences, Harvard University, 29 Oxford Street, Cambridge, MA 02138, USA*

Abstract

Atomic force acoustic microscopy is a dynamical AFM-based technique developed for non-destructive characterization of elastic properties of materials at micrometrical and sub-micrometrical scale. A standard AFM apparatus is equipped with a piezoelectric transducer exciting longitudinal oscillations at ultrasonic frequencies in the sample under investigation. Tip–sample contact stiffness is obtained through the values of the measured resonance frequencies of the cantilever contacting the sample surface, thus allowing one to obtain the value of the sample indentation modulus. The paper describes a generalization of the technique: while performing topography, the first and the second contact resonance frequencies are acquired at each point of the scanned area. Data are then properly processed and acoustic images are obtained as a bi-dimensional pattern of the indentation modulus over the imaged samples area. The technique is illustrated in two different kinds of sample: a metallographic (1 1 0) GaAs sample, prepared by incorporating GaAs single crystals into an epoxy matrix, and a diamond-like carbon film, deposited on a Mo substrate by laser ablation from a glassy carbon target.

PACS: 62.20.Dc; 68.37.Ps; 68.35.Iv

Keywords: Atomic force acoustic microscopy; Indentation modulus measurement; Elastic properties imaging

1. Introduction

In order to decrease the length scale in technological applications, one needs to develop instruments and techniques capable of characterizing material mechanical properties with sub-micrometrical spatial resolution. The use of standard micro- and nano-indentation tests for measuring the indentation modulus (Young's modulus for isotropic materials) at low scales is restricted mainly for three reasons: firstly the lateral resolution is limited by the size of the indenter; secondly, in case of thin films over a substrate, measurements are greatly affected by the very same substrate [1,2]; last but not least, such kind of measuring technique is often a destructive one rather than a non-destructive testing. In order to overcome these restrictions, AFM has been used alternatively as a statical [3,4] or a dynamical [5–9] indenter for non-destructive spot measurements of the indentation modulus at nanoscale. In particular, atomic force acoustic microscopy (AFAM) technique [6,9,10], which is a dynamical AFM technique based on the detection of the mechanical resonance frequencies of a vibrating cantilever, has been used to deduce sample elastic parameters from resonance frequencies shift in the two cases of free cantilever vibrating in air and cantilever vibrating in contact with the sample surface [1,9,10].

* Corresponding author.
E-mail address: daniele.passeri@uniroma1.it (D. Passeri).

0167-9317/$ - see front matter © 2006 Elsevier B.V. All rights reserved.
doi:10.1016/j.mee.2006.10.069

Moreover, AFAM images, as well as those obtained via the ultrasonic force microscopy (UFM) [11–13], *qualitatively* represent sample surface elastic properties [6,10,14,15]. Finally, an AFAM technique improvement has been recently proposed that, under suitable conditions, yields images that *quantitatively* reflect the elastic properties of sample surface, allowing the reconstruction of the local indentation modulus pattern on the sample surface to be done [16,17].

In this paper, the AFAM technique and the experimental apparatus are described. Firstly, in order to verify the reliability and the accuracy, AFAM measurements have been successfully performed on samples (Si, GaAs, InP, Al, and Pt) that have well known structural properties and whose indentation modulus is widely reported in literature. Then, two different samples are chosen in order to illustrate the technique's capability of retrieving acoustic images reflecting local elastic properties of sample surface. Such acoustic images are then processed, and the bi-dimensional pattern of the local indentation modulus of the sample surface is reconstructed.

2. Experimental

2.1. AFAM technique

In order to relate contact resonance spectra to sample local indentation modulus, the AFM cantilever can be modeled as a beam, with uniform rectangular cross section and length L, clamped at one end. The AFM tip, supposed to be placed at a distance L_1 from the cantilever clamped end, is brought into contact with the sample surface, that is set into vibration at ultrasonic frequencies through a piezoelectric transducer placed under the sample. For small surface vibration amplitudes, the tip–sample contact can be modeled as a linear spring whose elastic constant is the tip–sample contact stiffness k^* [6,9]. By modifying its boundary conditions, k^* determines the flexural resonance frequencies f_n's of the cantilever contacting the sample surface. From the measured frequencies set of contact resonance frequencies f_n's, contact stiffness k^* can be determined by the relation [6,9]

$$\begin{aligned} k^* = {} & \frac{2}{3}k_c\left(c_c\sqrt{f_n}r\right)^3 \times \left(1+\cos c_c\sqrt{f_n}\cosh c_c\sqrt{f_n}\right) \\ & /\left\{-\left(\cosh c_c\sqrt{f_n}r\sin c_c\sqrt{f_n}r-\sinh c_c\sqrt{f_n}r\cos c_c\sqrt{f_n}r\right)\right. \\ & \times\left(1+\cos(1-r)c_c\sqrt{f_n}\cosh(1-r)c_c\sqrt{f_n}\right) \\ & +\left(\cosh(1-r)c_c\sqrt{f_n}\sin(1-r)c_c\sqrt{f_n}\right. \\ & \left.-\sinh(1-r)c_c\sqrt{f_n}\cos(1-r)c_c\sqrt{f_n}\right) \\ & \left.\times\left(1-\cos c_c\sqrt{f_n}\cosh c_c\sqrt{f_n}\right)\right\}, \end{aligned} \tag{1}$$

where c_c is a characteristic parameter of the cantilever, k_c is the cantilever spring constant, and $r = L_1/L$ is used as a free fitting parameter. Experimentally, k^* and r can be deduced from the measured first and second contact resonance frequency, namely f_1 and f_2, by matching the expressions of k^* obtained at each mode [1] by imposing

$$k^*(f_1, r) = k^*(f_2, r). \tag{2}$$

The contact stiffness value k_s^* deduced on the tested sample is related to its reduced Young's modulus E_s^* through equation [6,9]

$$E_s^* = \frac{k_s^*}{2a}, \tag{3}$$

where a is the unknown tip–sample contact radius, that can be determined through calibration with a reference sample. Finally, the reduced Young's modulus allows one to determine sample indentation modulus M_s by the relation [6,9]

$$M_s = \left(\frac{1}{E_s^*} - \frac{1}{M_t}\right)^{-1}, \tag{4}$$

where M_t is the tip indentation modulus, e.g. $M_t = 164.8$ GPa for a (100) Si tip.

2.2. Experimental setup

The AFAM experimental apparatus (Solver P47H, NT-MDT, Russia) is a commercial AFM, equipped with a piezoelectric transducer, that excites longitudinal oscillations at ultrasonic frequencies in the sample under investigation [9]. Measurements were performed using commercial rectangular (100) silicon cantilevers (Mikromasch, nominal dimensions: length $L = 230 \pm 5$ μm, width $w = 40 \pm 3$ μm, and thickness $t = 7.0 \pm 0.5$ μm), whose spring constants k_c were previously estimated from first free resonance frequencies in air, according to the method of Sader et al. [18]. All the used tips have a flat apex shape, as highlighted by both AFAM and SEM characterization [9]. During AFAM experiments, harmonic components at ultrasonics frequencies present in the cantilever deflection signal, as a consequence of the oscillation of sample surface induced by the piezoelectric transducer, are detected by a lock-in amplifier. The obtained oscillation amplitude can be used as the AFAM signal and collected at each point of the scanned area, thus obtaining, in addition to topography, an acoustic image that qualitatively reflects the sample surface elastic properties [14]. Moreover, the resonance frequencies of the cantilever contacting sample surface can be measured at each point of the scan, and used as the AFAM signal. Actually, our experimental apparatus allows one to specify only one range for the detection of the resonance frequency during a single surface scan: consequently, two subsequent scans of the same area are required in order to obtain AFAM images at the first and second contact resonance frequencies. By numerically evaluating Eq. (2) at each point of the scanned area, the obtained AFAM images at f_1 and f_2 are processed and the indentation modulus pattern of the sample surface is reconstructed, provided that calibration of the tip on a (100) silicon single crystal, used as a reference sample, has been previously performed [17].

Please cite this article in press as: D. Passeri et al. Microelectr. Eng. (2006), doi:10.1016/j.mee.2006.10.069

3. Results and discussion

The reliability of this technique has been tested by measuring the indentation modulus of both isotropic and anisotropic samples, whose elastic properties are homogeneous on the surface and well known from literature. As a reference material, a (1 0 0) Si single crystal has been used, whose indentation modulus is given equal to $M_{Si} = 164.8$ GPa. The first and the second contact resonance frequencies were collected without scanning the surface, in order to prevent abrasion of the tip [9], and Eq. (2) was numerically solved, thus obtaining tip–sample contact stiffness values on test and reference samples, respectively. Through Eqs. (3) and (4), measured values of k_s^* have been used to obtain samples indentation modulus values, as listed in Table 1. Concerning the anisotropic samples, (1 0 0) GaAs and InP single crystals, the experimental indentation modulus values, M_{exp}, were compared to the indentation modulus values, M_{lit}, calculated from the c_{ij} elements of the elastic tensor through the method of the Green's function [9,19]. Concerning the isotropic samples (Al and Pt foils), Young's modulus E was evaluated from the indentation modulus M, through the relation

$$M = \frac{E}{1 - \nu^2}, \tag{5}$$

where ν is Poisson ratio. The experimental Young's modulus value E_{exp}, calculated from the measured M_{exp} through Eq. (5), has been compared with the value reported in literature, E_{lit}. Both ν and E_{lit} are supplied by the producer. The reported experimental error has been calculated on the basis of multiple measurements, performed using four different cantilevers, on both the reference (Si) and the investigated samples [9]. For all the four samples, experimental results were found to be in good agreement with the expected values, thus confirming the capability of AFAM technique to evaluate sample indentation modulus. As discussed above, acoustical images can be obtained that reflect elastic properties of sample surface by collecting the value of f_1 and f_2 at each point of the scan. AFAM images at f_1 and f_2 can be processed, by numerically evaluate Eq. (2) at each point of the scanned area, thus obtaining the reconstruction of the indentation modulus pattern on sample surface. In the following, two examples are reported, illustrating the technique for two different types of samples.

Table 1
Experimental indentation modulus values M_{exp} measured on both anisotropic and isotropic samples, using (1 0 0) Si single crystal as a reference sample, whose indentation modulus has been calculated as $M_{Si} = 164.8$ GPa

Sample	M_{exp} (GPa)	M_{lit} (GPa)	ν	E_{exp} (GPa)	E_{lit} (GPa)
GaAs	120 ± 12	117.5			
InP	93 ± 16	92.1			
Al	82 ± 11		0.35	72 ± 10	71
Pt	200 ± 30		0.39	170 ± 26	170

Concerning the anisotropic samples, (1 0 0) GaAs and InP single crystals, M_{exp} is compared to the calculated indentation modulus value reported in literature M_{lit}. Concerning the isotropic samples, Al and Pt foils, the experimental Young's modulus E_{exp} is evaluated as $E_{exp} = (1 - \nu^2)M_{exp}$, ν being Poisson ratio, and compared to value reported in literature, E_{lit}. Both ν and E_{lit} are supplied by the producer.

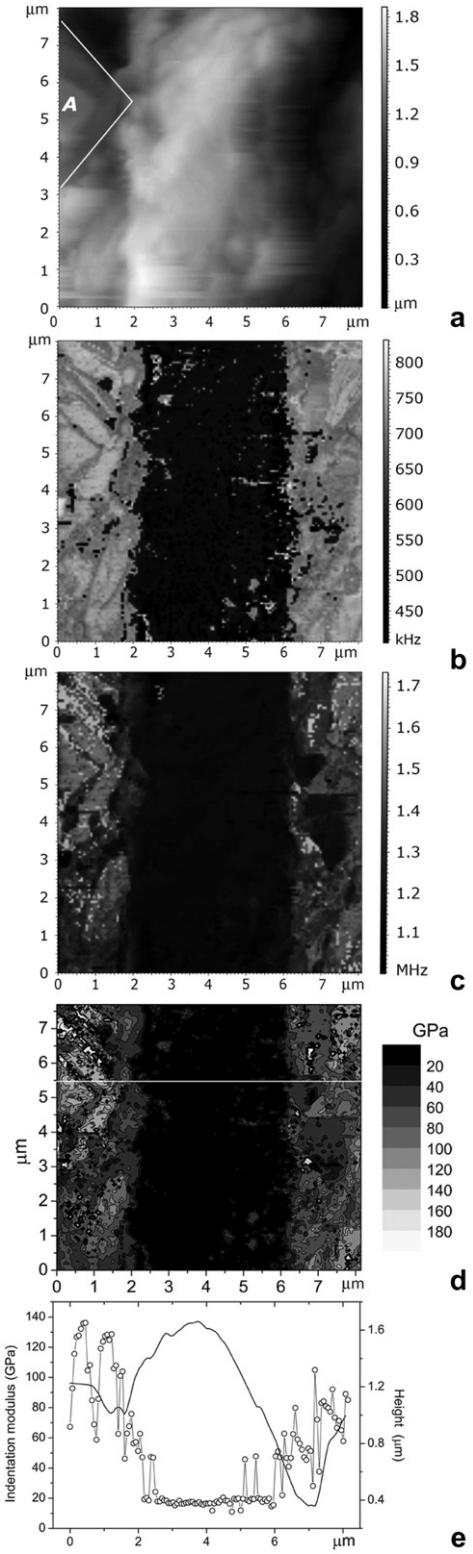

Fig. 1. AFAM characterization of a metallographic (1 1 0) GaAs sample incorporated in epoxy matrix: (a) AFM morphology; f_1 (b) and f_2 (c) AFAM images; (d) indentation modulus values pattern; (e) transversal section of profile height (solid line) and indentation modulus (open circles).

Fig. 1 shows topography and AFAM images of a metallographic (1 1 0) GaAs sample, prepared by incorporating GaAs single crystals into an epoxy matrix. The (1 1 0) surface was mechanically polished. The morphological characterization of the epoxy layer between two GaAs crystals (Fig. 1a), obtained through AFM in standard contact mode, does not show significant differences between the two materials. Fig. 1b and c have been obtained by measuring, at each point of the scanned area, the value of f_1 and f_2, respectively. In both AFAM images, a dark strip corresponding to lower contact resonance frequencies indicates the epoxy layer, whose indentation modulus is lower than that of GaAs. f_1 and f_2 AFAM images have been processed by numerically evaluating Eq. (2) at each point of the scanned area, thus reconstructing the local indentation modulus bi-dimensional pattern reported in Fig. 1d. The maximum experimental error in the evaluation of M was estimated as ±10%, on the basis of multiple measurements of k_s^* on the reference Si sample. The tip–sample contact radius, determined as $a = 12$ nm by AFAM measurement on the Si (1 0 0) reference sample, limits the lateral resolution of the technique [7,9]. Fig. 1e reports the values of both the indentation modulus and the profile height as measured along the line of Fig. 1d. Indentation modulus values obtained in correspondence of the epoxy layer do range between 14 GPa and 20 GPa. As far as it concerns the value of M_{GaAs} in the (1 1 0) crystallographic direction, the reconstructed pattern (Fig. 1d) is highly influenced by morphology, thus not allowing a correct evaluation of the indentation modulus to be done; nevertheless, referring to the flat portion of the surface marked with A in Fig. 1a, where morphology does not affect the indentation modulus pattern, the measured value of M ranges between 120 GPa and 135 GPa. Such a value is in good agreement with the calculated GaAs indentation modulus in the (1 1 0) crystallographic direction, $M = 125.1$ GPa, numerically evaluated from the c_{ij} elements of the stiffness tensor reported in literature [19,20].

As a second example, Fig. 2a shows the morphology of a diamond-like carbon (DLC) film, deposited on a Mo substrate at temperature $T_s = 400$ °C by laser ablation (excimer laser XeCl at $\lambda = 308$ nm, pulse duration 27 ns, frequency of pulses 3 Hz) from a glassy carbon (GC) target [17]. Fig. 2b and c are AFAM images at f_1 and f_2, respectively: dark agglomerates are clearly observable, indicating a decrease of indentation modulus with respect to the surrounding material. By processing Fig. 2b and c, the indentation modulus pattern reported in Fig. 2d is obtained [17]. The maximum experimental error in the evaluation of M was estimated as ±4%, on the basis of multiple measurements of k_s^* on the reference Si sample. The flat tip–sample contact radius has been determined as $a = 37$ nm, after the calibration in the Si (1 0 0) reference sample. A small increase of the contact radius a (from 36 nm to 37 nm), observed after 20 scannings of random areas of DLC sample surface, is due to abrasion of the tip [1,17]. Such a negligible effect is ascribable to the flatness of the apex, that involves low stress (0.3 GPa) between the tip and the DLC sample [17]. Moreover, the thickness of the DLC film, evaluated as 2 μm through standard profilometric

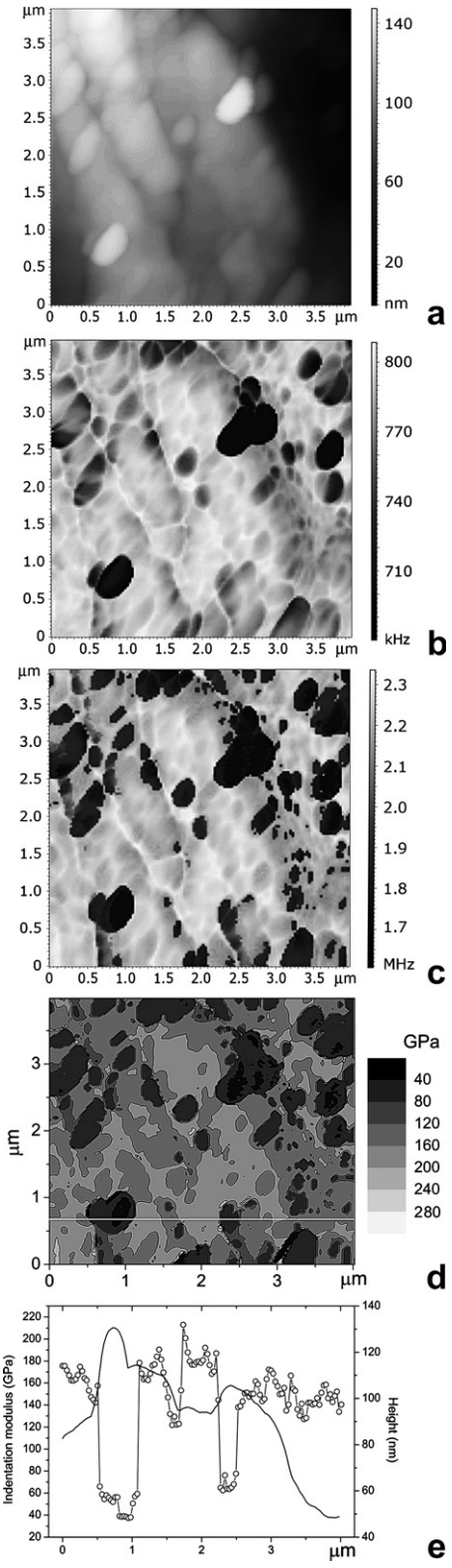

Fig. 2. AFAM characterization of a DLC film (See Ref. [17]): (a) AFM morphology; f_1 (b) and f_2 (c) AFAM images; (d) indentation modulus values pattern; (e) transversal section of profile height (solid line) and indentation modulus (open circles).

measurements (Profilometer Alpha Step, Tencor Instruments), allows one to neglect also the effect of the Mo substrate on AFAM measurements [7]. Finally, Fig. 2e reports the values of both the indentation modulus and the profile height as measured along the line in Fig. 2d. Indentation modulus of the film surrounding the agglomerate ranges between 140 GPa and 180 GPa, corresponding to a DLC film with low sp^3/sp^2 hybridization ratio [17]. The indentation modulus value of the dark agglomerate is $M = 41 \pm 4$ GPa, compatible with the indentation modulus measured on the GC target [17]: the observed agglomerates correspond to amorphous carbon ablated from the GC target and deposited on the substrate, with no bond rearrangement [17].

4. Conclusions

In conclusion, the AFAM technique has been proved to be a powerful tool that may retrieve information on the indentation modulus of the sample surface with sub-micrometrical spatial resolution. Acoustic images reflecting the elastic properties of the sample surface have been obtained by acquiring, simultaneously to topography, the first and the second tip–sample contact resonance frequencies. These images have been processed, obtaining a quantitative reconstruction of the local indentation modulus of the sample surface. AFAM based on the two frequencies imaging technique is proposed as a promising investigation tool for the mechanical characterization of nano-structured materials.

Acknowledgements

The authors gratefully acknowledge F. Stella and C. Palazzesi for the profilometric measurements on the DLC sample. G. Zollo is acknowledged for providing the metallographic GaAs sample.

References

[1] S. Amelio, A.V. Goldade, U. Rabe, V. Scherer, B. Bhushan, W. Arnold, Thin Solid Films 392 (2001) 75.
[2] M. Kopycinska-Müller, R.H. Geiss, J. Müller, D.C. Hurley, Nanotechnology 16 (2005) 703.
[3] A.L. Weisenhorn, M. Khorsandi, S. Kasas, V. Gotzos, H.J. Butt, Nanotechnology 4 (1993) 106.
[4] C. Reynaud, F. Sommer, C. Quet, N. El Buonia, T. Minh Duc, Surf. Interface Anal. 30 (2000) 185.
[5] E. Dupas, G. Gremaud, A.J. Kulik, J.L. Loubet, Rev. Sci. Instrum. 72 (2001) 3891.
[6] U. Rabe, J. Janser, W. Arnold, Rev. Sci. Instrum. 67 (1996) 3281.
[7] E. Kester, U. Rabe, L. Presmanes, P. Tailhades, W. Arnold, J. Phys. Chem. Solids 61 (2000) 1275.
[8] D.C. Hurley, K. Shen, N.M. Jennett, J.A. Turner, J. Appl. Phys. 94 (2003) 2347.
[9] D. Passeri, A. Bettucci, M. Germano, M. Rossi, A. Alippi, S. Orlanducci, M.L. Terranova, M. Ciavarella, Rev. Sci. Instrum. 76 (2005) 093904.
[10] U. Rabe, S. Amelio, E. Kester, V. Scherer, S. Hirsekorn, W. Arnold, Ultrasonics 38 (2000) 430.
[11] O. Kolosov, K. Yamanaka, Jpn. J. Appl. Phys., Part 2 32 (1993) L1095.
[12] F. Dinelli, S.K. Biswas, G.A.D. Briggs, O. Kolosov, Phys. Rev. B 61 (2000) 13995.
[13] L. Muthuswami, R.E. Geer, Appl. Phys. Lett. 84 (2004) 5082.
[14] U. Rabe, S. Amelio, M. Kopycinska, S. Hirsekorn, M. Kempf, M. Göken, W. Arnold, Surf. Interface Anal. 33 (2002) 65.
[15] U. Rabe, E. Kester, W. Arnold, Surf. Interface Anal. 27 (1999) 386.
[16] D.C. Hurley, M. Kopycinska-Müller, A.B. Kos, R.H. Geiss, Meas. Sci. Technol. 16 (2005) 2167.
[17] D. Passeri, A. Bettucci, M. Germano, M. Rossi, A. Alippi, V. Sessa, A. Fiori, E. Tamburri, M.L. Terranova, Appl. Phys. Lett. 88 (2006) 121910.
[18] J.E. Sader, J.W.M. Chon, P. Mulvaney, Rev. Sci. Instrum. 70 (1999) 3967.
[19] J.J. Vlassak, M. Ciavarella, J.R. Barber, X. Wang, J. Mech. Phys. Solids 51 (2003) 1701.
[20] J.S. Blakemore, J. Appl. Phys. 53 (1982) R123.

Please cite this article in press as: D. Passeri et al. Microelectr. Eng. (2006), doi:10.1016/j.mee.2006.10.069